

Electronic Supplementary Information

Immobilization of Hexa-Arginine Tagged Esterase onto Carboxylated Gold Nanoparticles

Tai Hwan Ha,¹ Jin Young Jeong,² Bong Hyun Chung^{1,2*}

¹BioNanotechnology Research Center, Korea Research Institute of Bioscience and Biotechnology and ²University of Science and Technology, P. O. Box 115, Yuseong, Daejeon 305-600, Korea

S.1 ATR-IR analyses of the esterase immobilized on AuNP-COOH In Fig. S1, the detailed structural characteristics of the Arg₆-esterase immobilized on the surface of AuNP-COOH was investigated by FTIR-ATR measurements. The presence of small amount of esterase on AuNP-COOH was easily detected owing to the multiple reflections of ATR mode (12 reflections).¹ The buffered AuNP-COOH solution was exchanged with distilled water (DW, pH 6.2) through centrifugation and re-dispersion cycle twice to avoid interferences from buffer molecules. The resulting AuNP-COOH solution with distilled water was dropwisely spread on ATR element and dried under N₂ stream. The AuNP-COOH spread on the ATR element showed C=O stretching band at 1710 cm⁻¹ in its dimer state along with the shoulder near 1740 cm⁻¹ that can be considered as a monomer state. The broad features ranging from 1700 cm⁻¹ to 1550 cm⁻¹ were assigned by curve fitting as oligomeric and hydrogen bonded C=O stretching at 1689 cm⁻¹, OH bending mode of adsorbed water molecules in liquid state at 1648 cm⁻¹, and COO⁻ asymmetric stretching band at 1545 cm⁻¹.² Since C=O stretching mode has a quite comparable dipole moment with COO⁻ asymmetric band, carboxyl groups on the

AuNPs seem to exist mostly in a neutral state. The lower deprotonation level compared to pK_a values of several fatty acids (~ 4.7) was presumably attributed to the effect of surface confinement, but much more deprotonation might occur in the working pH 8.0.^{2,3}

The infrared spectral feature of methylene groups in MHA is also very informative since their peak positions indicate the chain conformation of long MHA chains (inset of Fig. S1).^{4,5} The peak frequencies 2918 cm^{-1} and 2849 cm^{-1} , assigned as CH_2 asymmetric and symmetric stretching bands, designates all-trans alkyl chains with minimal gauche conformation.⁵ Water dispersible and highly stable characteristics of the present AuNPs might be attributed to the well close-packed alkyl chains serving as a physical barrier against the formation of particle agglomerates. Soaking the AuNP-COOH with esterase resulted in two distinct peaks at 1658 cm^{-1} and 1540 cm^{-1} , which were proportional to the amount of esterase. These bands in Fig. S1, which are normalized by equalizing the CH_2 asymmetric bands in each spectrum, can be assigned as amide I and II bands of esterase.^{6,7} The adsorption of esterase hardly changed the CH_2 stretching bands of MHA, demonstrating the robustness of the MHA modification and the interaction of hexa-arginine with surface confined carboxyl groups.

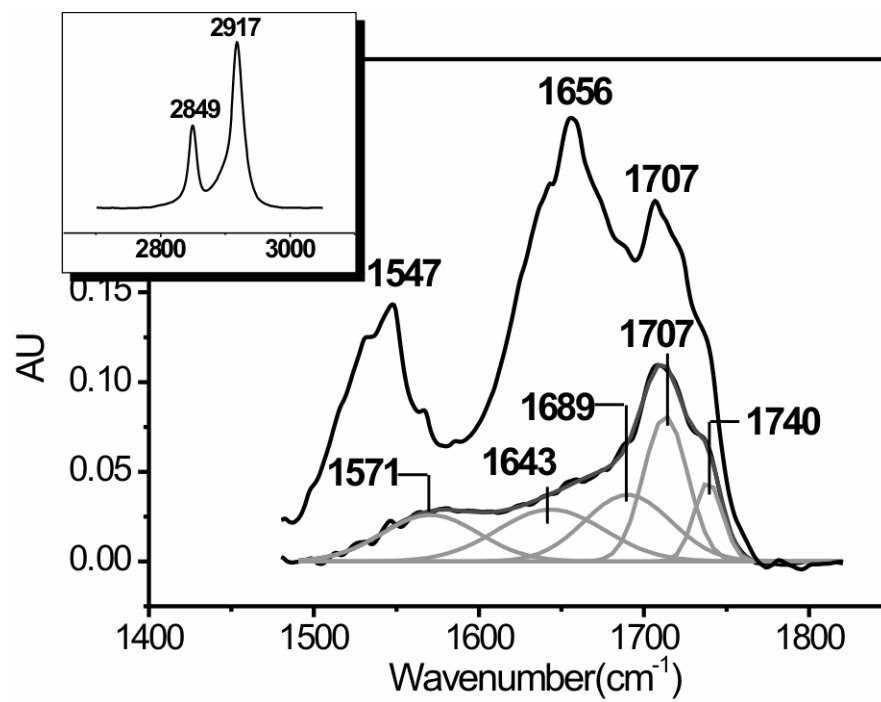


Fig. S1

S.2 Measurements for enzyme kinetics

Besides the changes of protein conformation, diffusional limitation faced when the reaction rate of an enzyme is mainly determined by the supply of the substrate, might be one of other minor origins of the reduced activity (i.e. 58% for Arg₆-esterase). The present esterase-AuNP complex can be considered as an extreme case of the entrapped or surface-bound enzyme systems.⁸ However, the particle radius of the present AuNP was very small compared to the conventional supporting beads (~ 10 μm). From a simple calculation of root-mean-square distance diffused by pNPB in water ($R_{\text{rms}} = (6D_0t)^{1/2}$, $D_0 = 5.0 \times 10^{-6} \text{ cm}^2/\text{s}$:assumed, t in second), pNPB molecules was calculated to travel 5.5 μm in a second.⁹ On the other hand, the depletion radius of pNPB consumed by twenty esterases densely packed in a single position, was estimated at best 600 nm by considering working concentration (0.1 mM) and the specific enzyme activity value for the present esterase (38,500 μmol pNPB/s·mg protein, *ref. 11* in the ESI).

This conclusion could be further justified by a kinetic experiment assuming Michaelis-Menten type enzyme kinetics for the present system. The absorbance value at 400 nm, which increases as pNPB is dissociated by the enzyme, was used as a marker for the kinetic experiments. As illustrate in Fig. S2, the initial rates for four different pNPB concentrations (>0.05 mM) were obtained by monitoring the absorbance changes. According to Michaelis-Menten kinetics, the reaction rate can be described as follows; $rate = d[P]/dt = V_m[S]/(K_m + [S])$, $[S]$: substrate, $[P]$: product. In the double reciprocal plot, the inverse of the reaction rates are plotted versus the inverse of the initial concentration of the substrate as shown in Fig. S3. The amounts of enzymes for both free and immobilized are leveled to a similar value, but the exact values were different

according to the subsequent quantifications by SDS-PAGE. As shown in Fig. S3 in the ESI, both free and bound esterases had the same K_m values (minus inverse of x -intercepts) in the plot. Accordingly, the esterases on the surface of AuNP can be concluded not to be restricted by the substrate diffusion at the working concentration ($\sim 0.1\text{mM}$).⁸

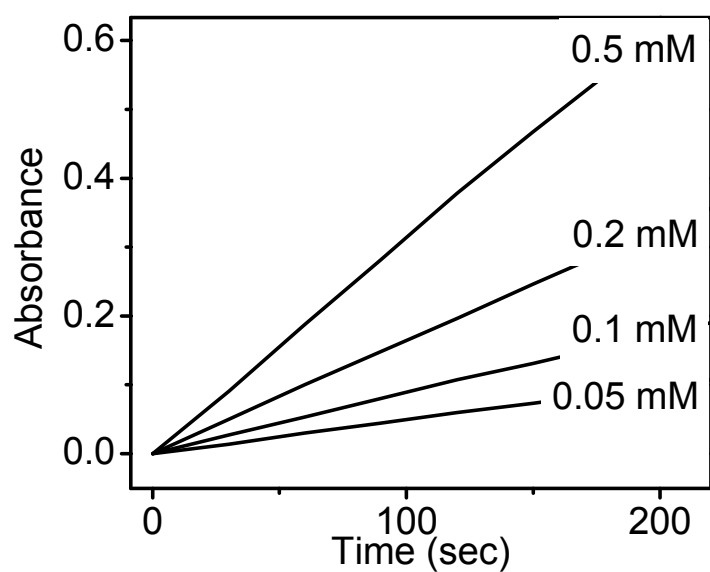


Fig. S2

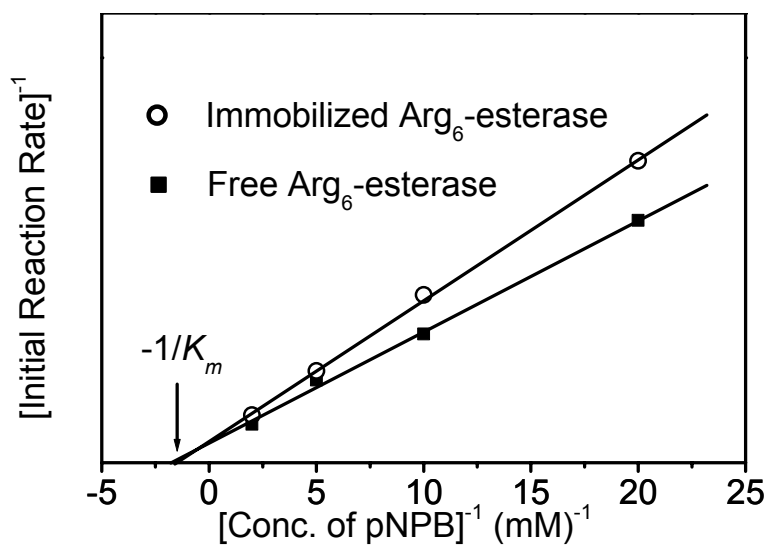


Fig. S3

Concentration (mM)	Absorbance at 120s (for free esterase)	Absorbance at 120s (for immobilized esterase)
0.5	0.4676	0.3780
0.2	0.2179	0.1963
0.1	0.1396	0.1072
0.05	0.0742	0.0596

Table S1

S.3 Experimental Details

Chemicals HAuCl₄·3H₂O (99.9%), citric acid (trisodium salt 99%), and 16-mercaptohexadecanoic acid (MHA, 90%) were purchased from Aldrich and used as received. Bovine serum albumin and *p*-nitrophenol butyrate (pNPB, 99%) was purchased from Sigma, and recombinant none-tagged (yield: 55%), hexa-histidine tagged (His₆-tagged, yield: 90%), and six arginine tagged (Arg₆-tagged, yield: 50%) esterases were purchased from Bioprogen (Korea).^{10,11} The tags were attached on the N-terminal of the protein and the detailed procedures for manufacturing recombinant proteins are described in the later section. All the solvent otherwise specified were reagent grade, and triply distilled water of resistivity greater than 18.0 MΩ·cm was used in making aqueous solutions.

AuNP synthesis The aqueous AuNP was prepared by following the procedures described in the literature:¹² 120 mg of HAuCl₄ was initially dissolved in 250 mL of water, and the solution was brought to boiling. A solution of 1% sodium citrate (50 mL) was then added to the HAuCl₄ solution under vigorous stirring, and boiling was continued for *ca.* 60 min. Then, the AuNP solution was cooled down to room temperature and final volume was adjusted to 250 ml with distilled water, which resulted in the AuNP concentration of 18 nM. The resulting deep red solution showed the characteristic surface plasmon band at 522 nm and Average diameter of AuNP was determined to be 13 ± 2 nm from TEM image.

MHA modification of AuNP and enzyme immobilization Since MHA molecules are not soluble in an aqueous solution, ethanol solution containing MHA of 5 mM was dropwisely added to the AuNP solution to make a final concentration of 0.6 mM. The AuNP solution was heated up to 90 °C during the addition of MHA without any surfactant, which is often used to avoid particle aggregation (as in the *ref.* 13 of the manuscript). Mild heating was continued for 2 hours and the solution was cooled down to room temperature. After aging for 24 hours at room temperature, insoluble precipitate of MHA was removed by extraction with chloroform and again adjusted to the initial volume with distilled water. Enzyme immobilization was carried out by soaking the AuNP-COOH with esterase solution (0.2 mg/ml, 50 mM Tris buffer, pH 8.0) for 2 hours. Adsorbed protein on AuNP-COOH was separated from unbound one by centrifugation and re-dispersed in buffer solution or distilled water for further characterizations.

UV/Vis spectral measurement UV/Vis spectra were recorded for AuNP solution using DU-800 spectrophotometer (Beckman Coulter) with a quartz cell with 1 cm path

length. For quantitative measurements, concentrations of AuNP solution were adjusted to a constant value by monitoring absorbance at ~525 nm.

FTIR measurements Infrared spectra of the above samples were obtained by using a Bruker IFS 113V FT-IR spectrometer equipped with a Specac ATR attachment, and a liquid-N₂-cooled mercury-cadmium-telluride detector. The incident angle of infrared light was set at 45 with respect to the plane of the ZnSe crystal such that 12 internal reflections in total took place throughout the crystal. The 128-times-scanned interferograms were collected at 4 cm⁻¹ resolution.

TEM analyses TEM images were acquired for AuNPs using a JEM-200CX transmission electron microscope at 120 kV. TEM samplings were accomplished by loading a droplet of AuNP solution onto Formvar-coated copper grids (200 mesh), drying for 5 min in laboratory atmosphere, and washing off the excess solution with N₂ blowing.

Sodium dodecyl sulfate poly(acrylamide) gel electrophoresis analyses SDS-PAGE gels were prepared at 12% and 5% of poly(acrylamide) concentrations for separating and stacking gels, respectively. Loading wells were formed by placing a comb and concentrated nanoparticle solutions with adsorbed esterase (10 ul) were loaded. For a typical experiment, constant voltage of 200 V was applied for 1 h. Then, gels were placed in staining solution (0.5% Coomassie blue, 45% methanol, 10% acetic acid aqueous solution) for 30 min, followed by destaining solution (10% methanol, 10% acetic acid aqueous solution) for 3 h, and scanned on a flatbed scanner.

Enzyme activity assay The enzymatic activities of esterase were assayed by UV/Vis spectra of absorption characteristics in the enzymatic substrate, *p*-nitrophenol butyrate (pNPB, 0.1mM). The substrate soaked with the enzyme solution quickly dissociates into nitrophenol, which develops a new absorption band at 400 nm. Therefore, the spectral changes at 400 nm can be a good indicator of enzyme reaction. In order to avoid the interference from large surface plasmon band from AuNP, the reaction vessel containing the supported esterase on AuNP and pNPB was quenched in an icebox (0 °C) immediately after a predetermined reaction time. Then, AuNP with esterase was removed by centrifugation at 17500 g (4 °C) for 15 min, and the absorbances of the supernatant were recorded by the UV/Vis spectrometer. In contrast, for Arg₆-tagged esterase, which showed high enzymatic activity even on AuNP-COOH, direct observation was carried out since sixteen times diluted solution used. In addition, it was claimed and separately confirmed in our laboratory that affinity tagging hardly affected the enzymatic activities.

Construction of expression vectors The esterase gene was acquired from *Pseudomonas* sp. KCTC10122BP and detailed method can be found elsewhere.^{10,11} The esterase genes were PCR-amplified using *pfu* polymerase (Bioprogen, Korea) and sets of synthetic primers (For none-tagged esterase: N-terminal 5'-GGCCA TATGC AGATT CAGGG ACATT ACGAG CTT-3' and C-terminal 5'-GGCCT CGAGT TACAG ACAAG TGGCT AGTAC CCG-3'. For His₆-esterase: N-terminal 5'-GGCCA TATGC ACCAC CACCA CCACC ACATG CAGAT TCAGG GACAT TACGA G-3' and C-terminal 5'-GGCCT CGAGT TACAG ACAAG TGGCT AGTAC CCG-3'. For Arg₆-esterase: N-terminal 5'-GGCCA TATGC GCCGC CGCCG CCGCC GCCAG ATTCA GGGAC ATTAC-3' and C-terminal 5'-GGCCT CGAGT TACAG ACAAG TGGCT AGTAC CCG-3'). The restriction sites, *Nde*I and *Xho*I (underlined sequences), were introduced into the N- and C-terminal primers, respectively. The amplified DNA fragment (1.2 kb) was purified and subcloned into the *Nde*I/*Xho*I sites of pET22b(+) (Novagen, Germany). The resulting vector constructs were designated pETESTa (none-tagged), pET6HESTa (His₆), and pET6RESTa (Arg₆), respectively, and confirmed by DNA sequencing.

Overexpression and purification of esterases For none-tagged and His₆-esterases, *E.coli* BL21 (DE3) (Stratagen, USA) was transformed with pETESTa and pET6HESTa, respectively, while *E.coli* Rosetta *gami* (DE3) (Stratagen, USA) was used for Arg₆-esterase (pET6RESTa). The transformed cells were cultured in Luria-Bertani (LB) media and allowed to grow at 30 °C to OD 0.6 before the IPTG induction (1 mM) of recombinant proteins. After the culture broths were incubated overnight at 25 °C, *E.coli* cells were harvested by a centrifugation and subsequent washes with buffer (50 mM Tris-HCl, 10 mM EDTA, pH 8.0, twice). The resulting pellets were re-suspended in 50 ml extraction buffer (50 mM Tris-HCl, pH 8.0) and disrupted using a sonicator (Sonics & Materials, USA). The soluble fractions, obtained after centrifugation at 12,000 rpm for 20 min, were clarified with a membrane filter (Millipore, USA).

For none-tagged and Arg₆-esterases, the supernatants were loaded onto a Q Excellose ion-exchange column (2.5 cm x 30 cm, Millipore, USA) and the bound proteins were washed with the equilibration buffer (50 mM Tris-HCl, pH 8.0). The bounded target proteins were eluted with a linear gradient of NaCl from 0 to 1M at a flow rate of 4 ml/min. Each of the eluted fractions was subjected to SDS-PAGE (12%) and activity analysis to estimate production yield. The resulting main eluents were collected and dialyzed against 50 mM Tris-HCl buffer (pH 8.0).

For His₆-esterase, the soluble fraction was loaded onto IDA Excellose affinity column (2.5 cm x 30 cm, Millipore, USA). The bound protein was washed with the

equilibration buffer (50 mM Tris-HCl, 0.5 M NaCl, pH 8.0, twice) and eluted with a linear gradient of imidazole from 0 to 0.5 M at a flow rate of 4 ml/min. Each of the eluted fractions was subjected to SDS-PAGE (12%) and activity analysis to estimate production yield. The resulting main eluents were collected and dialyzed against 50 mM Tris-HCl buffer (pH 8.0).

1. Lee, M. H.; Ha, T. H.; Kim, K. *Langmuir* **2002**, 18, 2117.
2. Gershevit, O.; Sukenik, C. N. *J. Am. Chem. Soc.* **2003**, 126, 482-483.
3. Kakiuchi, T.; Iida, M.; Imabayashi, S.; Niki, K. *Langmuir* **2000**, 16, 5397-5401.
4. MacPhail, R. A.; Strauss, H. L.; Snyder, R. G.; Elliger, C. A. *J. Phys. Chem.* **1984**, 88, 334.
5. Gericke, A.; Huhnerfuss, H. *Thin Solid Films* **1994**, 245, 74-85.
6. Ding, F.; Xie, H.; Arshava, B.; Becker, J. M.; Naider, F. *Biochemistry* **2001**, 40, 8945-8954.
7. Mars, D.; Müller, M.; Schmitt, F. *Biophys. J.* **2000**, 78, 2499-2510.
8. Shuler, M. L.; Kargi, F. In *Bioprocess Engineering Basic Concepts*; Prentice-Hall Inc.: New York, 1992; pp 58-102.
9. Mortimer, R. G. In *Physical Chemistry*; The Benjamin/Cummings Publishing Company Inc.: New Jersey, 1993; pp 708-747.
10. Lee, E. G.; Won, H. S.; Ro, H.; Ryu, Y.; Chung, B. H. *J. Mol. Catal. B* **2003**, 26, 149.
11. Kim, G. J.; Lee, E. G.; Gokul, B.; Hahm, M. S.; Prerna, D.; Choi, G. S.; Ryu, Y. W.; Ro, H. S.; Chung B. H. *J. Mol. Catal. B* **2003**, 22, 29.
12. Lee, P. C.; Meisel, D. *J. Phys. Chem.* **1982**, 86, 3391.